

**Master's Thesis**



**F3** Faculty of Electrical Engineering  
Department of Computer Graphics and Interaction

**SIMR**

**Simulating the phenomena of altered states of consciousness using virtual reality**

**Jakub Hlusička**

**2021–2022**

**Supervisor: Ing. Josef Kortan**



Diplomová práce



**F3** Fakulta elektrotechnická  
Katedra počítačové grafiky a interakce

**SIMR**

**Simulace fenoménů pozměněných stavů  
vědomí pomocí virtuální reality**

Jakub Hlusička

**2021–2022**

Školitel: Ing. Josef Kortan



# Abstract

TODO

## Acknowledgements

TODO thank sci-hub

—Jakub Hlusička

*“Not everything that is faced can be changed, but nothing can be changed until it is faced.”*

—James Baldwin, As Much Truth as One Can Bear (1962)

# Contents

<b>1</b>	<b>Implementation</b>	<b>1</b>
1.1	Design of the Application . . . . .	1
1.1.1	Safety . . . . .	1
1.1.2	Interaction . . . . .	2
1.1.3	Virtual Scene Creation . . . . .	2
1.2	Implementation of Replications . . . . .	4
1.2.1	Spatial Effects . . . . .	4
1.2.1.1	Depth Perception Distortion . . . . .	4
1.2.1.1.1	First Attempt . . . . .	4
1.2.1.1.2	Final Solution . . . . .	6
1.2.1.2	Visual Drifting . . . . .	10
1.2.2	Non-Spatial Effects . . . . .	11
1.2.2.1	Visual Acuity Enhancement . . . . .	11
1.2.2.2	Tracers . . . . .	11
1.3	Complex Replication . . . . .	12
1.3.1	Execution Order . . . . .	12
1.3.2	Experiment Automation . . . . .	12
	<b>Bibliography</b>	<b>16</b>

# 1 | Implementation

The objective of this part of the project was to implement an immersive replication of altered states of consciousness (**ASCs**) induced by classical psychedelics. In order to achieve a high degree of immersion, our solution was designed to be intended for immersive virtual reality (**VR**) systems with head-mounted displays (**HMDs**). Our solution will be referred to with “*the application*” or “*our application*” for the rest of this document.

To represent the **ASCs** of classical psychedelics objectively, we had to resort to modelling only the “perceptual level” stage of the psychedelic experience (as seen in figure ??), as further stages require subjective personalization of content, and aspects less suitable for replication via immersive **VR**, such as cognitive effects and the suppression of the *phenomenological ego*.

## 1.1 Design of the Application

The application was designed primarily for the evaluation of the implemented replication. The development of the application consisted of 3 distinct parts:

1. **The environment:** A virtual scene that should look as realistic as possible.
2. **The replication:** Implementation of the effects themselves.
3. **Adaptation for testing:** Getting the application ready for a study, that might measure the impact of the replication on the human mind.

### 1.1.1 Safety

In order to ensure our application’s users safety, we have consulted the *Recommendations for good scientific practice and the consumers of VR-technology* (Madary and Metzinger 2016). The application was developed according to these recommendations.

Mainly, we don’t expect the developed application to have lasting traumatic effects on the users; instead, we believe that this medium may be a suitable way to explore aspects of psychedelic-induced **ASCs** while minimizing those risks.

Further, we’ve taken safety and intuitiveness into account while designing the controls and choosing a suitable testing area for experimentation with **VR** (the

“VR play space”).

Finally, the application must be automated, so that the administrator may assist the user and ensure their safety during the usage of the application.

### 1.1.2 Interaction

Interaction with the scene via hand-held controllers was removed entirely, as we felt that the currently available consumer VR technology does not implement a realistic, consistent, universal and intuitive solution for interaction with the virtual scene. For example, in VR applications, interactions are usually implemented so that if a user takes a hand-held controller to a dynamic physics-enabled object, they may be able to pick it up by pressing or holding a trigger on the hand-held object, which makes the object stick or snap to the virtual representation of the controller in the scene. While this solution may be suitable for VR games, it is still understood as a simplification.

As an alternative, one may consider using force feedback haptic gloves, and given a sufficient physically based simulation, it may be possible to implement realistic interactions with virtual objects. However, even such gloves apply force feedback only to the fingers and not the entire body, making it impossible to, for example, lean against virtual objects.

In any case, no such force feedback haptic gloves were available to us for this project, and so interaction was entirely foregone, in the interest of keeping the simulation focused mainly on the replication, rather than an unrealistic implementation of interactions.

### 1.1.3 Virtual Scene Creation

Given the goal of creating as realistic of a scene as possible, as well as no financial budget for this project, we ended up choosing Unreal Engine 4 (UE4)<sup>1</sup> as the game development engine to develop our VR application with. UE4 is free to use for projects with a lifetime gross revenue below \$1 million USD, and we have no plans to monetize it. Additionally, the choice of UE4 makes it possible to use the Quixel Megascans<sup>2</sup> 3D asset library for free within UE4, due to special licensing as a result of the acquisition of Quixel by Epic Games<sup>3</sup>, the developer of UE4.

The virtual scene was created with the intended VR play space in mind, which was measured to be about  $3.5 \times 3.5 \text{ m}^2$  large. The virtual scene contains visual cues of the play area borders in the form of 3D assets; specifically, the play area is surrounded by a railing and tall rock, communicating to the user, that these objects should not be passed through.

The choice was made to create an outdoor scene, as the surrounding nature might

---

<sup>1</sup><https://web.archive.org/web/20220514231756/https://www.unrealengine.com/en-US>

<sup>2</sup><https://web.archive.org/web/20220514233901/https://quixel.com/megascans>

<sup>3</sup><https://web.archive.org/web/20220514235540/https://www.epicgames.com/site/en-US/home>

provide a more pleasant environment than an indoor scene. However, our implementation is in no way limited to outdoor scenes only.

At first, we attempted to create a forest scene, but quickly ran into performance issues while trying to render a densely populated forest on a **HMD**, which requires at least 2 views rendered at typically higher resolutions than a regular desktop screen, ideally with at least 90 **FPS** (the native refresh rate of the **HMD**). Delivering a consistent framerate is a requirement, as low framerates and stuttering may cause motion sickness.

It was then decided to abandon the idea of a forest scene and, instead, use a high dynamic range imaging (**HDRI**) panoramic photograph as a background (hereinafter “panoramic background”) for the scene. It is important to note, that a panoramic background has no depth information. This drawback can be mitigated by making only the very distant parts of the panoramic background visible to the user, so that the illusion of the panoramic background being realistic is not broken. The illusion relies on the fact that binocular disparity is low for distant objects.

Close parts of the panoramic background can be hidden with 3D assets suitable for the environment. To minimize the area that needed to be hidden, we have chosen a mountainside panoramic background (see figure 1.1).



**Figure 1.1:** The chosen panoramic background “Cannon”<sup>4</sup> available on **Poly Haven**<sup>5</sup>.

The final scene contains a flat patch of grass and other low foliage the size of the *play area*, containing a wooden bench with some gardening tools. The grass patch is surrounded with rock formations and a rocky stairway leading towards it. Beyond the railing, there is a nice view of the sea cove.

---

<sup>4</sup>Released by Greg Zaal under the [CC0 1.0](#) (public domain) license.

<sup>5</sup><https://web.archive.org/web/20220515010919/https://polyhaven.com/a/cannon>

TODO: image of the scene

**Figure 1.2:** A preview of the resulting scene.

## 1.2 Implementation of Replications

The following replications are modelled after surveys of the phenomenology of psychedelic states (Preller and Vollenweider 2016; Kometer and Vollenweider 2016) and personal reports (Kleinman, Gillin, and Wyatt 1977).

### 1.2.1 Spatial Effects

The spacial effects of this section are a form of a vertex shader, or part thereof. UE4 has a concept of so-called “materials” – assets that can be applied to meshes to control the visual look of 3D assets. UE4 materials are defined using a built-in visual programming node graph. While this approach of specifying graphics processing unit (GPU) shader logic allows for tighter integration with UE4’s rendering engine and its lighting model, it makes it difficult to use conventional shading languages such as OpenGL Shading Language (GLSL) or High Level Shading Language (HLSL). The usage of conventional shading languages is sometimes desirable, because the provided material node graph editor cannot, by design, express some control flow constructs, such as loops.

However unwieldy, it is possible to use HLSL code in material graphs, in UE4. The directory of our custom HLSL shader files must be properly registered in the engine via an engine plugin (Alessa Baker 2021). The shader files can then be referenced from within “custom” nodes of the material node graph editor.

#### 1.2.1.1 Depth Perception Distortion

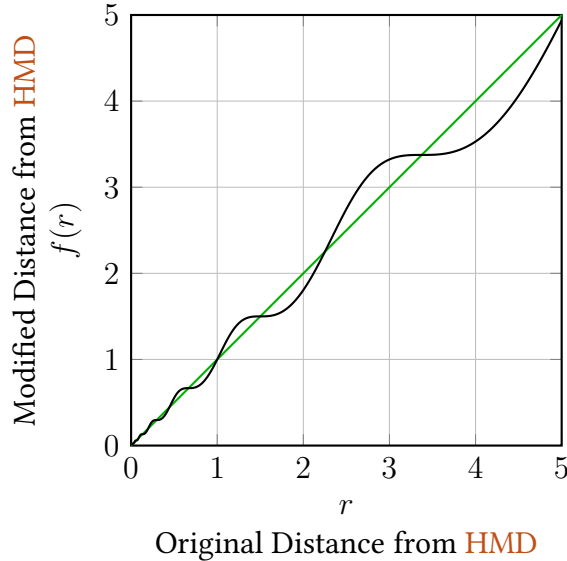
This replication simulates the distorted perception of depth, micropsia, and macropsia (Fischer et al. 1970; Dittrich 1998; Hill, Fischer, and Warshay 1969; Hill and Fischer 1973).

**1.2.1.1.1 First Attempt** Our first attempt made use of a self-similar, bijective and continuous function  $f$  to modify the distance of vertices from the HMD. The self-similarity is required to ensure that no self-intersection of geometry occurs, after the offset has been applied.

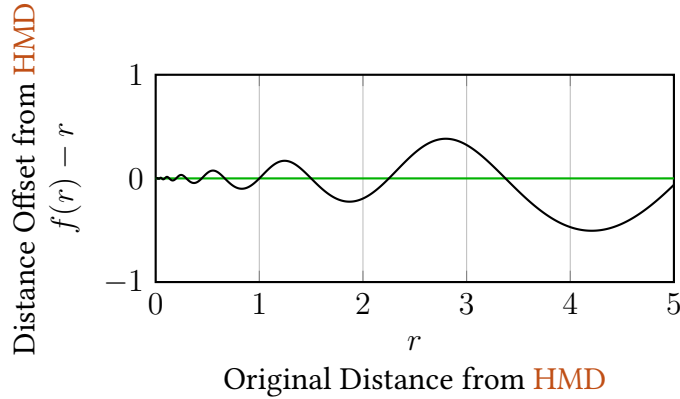
$$f(r) = a^{\frac{1}{\pi}} \sin(\pi \log_a r) + \log_a r \quad (1.1)$$

Where  $a \in (1; +\infty)$ .

The interesting property of self-similarity results in the maximum offset being directly proportional to the distance of the HMD. The graph of the function can be seen in figure 1.3.



(a) Modified distance from the **HMD**. Green line corresponds to the identity function for reference.



(b) Distance offset from the **HMD**. Green line corresponds to the X axis for reference. Note that the maximum distance offset is directly proportional to the distance from the **HMD**.

**Figure 1.3:** First attempt at distorting depth perception, unused in the final application. The function  $f$  from equation 1.1 modifies the distance of vertices from the **HMD**. Parameter  $a = 1.5$ .

Although this first iteration resulted in visually enticing results, we also noticed that it caused motion sickness in **VR**, particularly during the user's movement. We believe the motion sickness was caused by clusters of geometry moving with the position of the **HMD**, as if attracted to it, and caused a discrepancy between the user's vestibular system and the visual information.

Another disadvantage of this solution is its predictability and the synthetic look caused by its uniformity.

**1.2.1.1.2 Final Solution** In order to break up clusters of similarly affected geometry, we decided to use procedural noise. Procedural noise has been used for the generation of textures (Perlin 1985), and would be suitable to create a less predictable, more chaotic effect.

There are various kinds of procedural noise used in computer graphics. We found Simplex noise (Olano et al. 2002) to be suitable for our use-case, particularly for its  $\mathcal{O}(n^2)$  time complexity in  $n$  dimensions, lack of directional artifacts (visual isotropy), and a well-defined continuous gradient.

Let's denote the simplex noise sampling function as  $s: \mathbb{R}^n \rightarrow \mathbb{R}$ .

Now that we have a way to sample the noise, we could try to use the noise sample (possibly scaled by a constant) as the offset of the distance of each vertex to the HMD, as shown in the previous section. To retrieve the sample, we can use:

$$s' := s \begin{pmatrix} f_s x \\ f_s y \\ f_s z \\ f_t t \end{pmatrix} \quad (1.2)$$

where  $s'$  is the resulting sample,  $x, y$  and  $z$  are spacial coordinates of any point in space (typically the position of a vertex),  $t$  is the current time in seconds, and  $f_s$  and  $f_t$  are space-wise and time-wise frequencies of the noise, respectively.

With the addition of the time coordinate, resulting in 4-dimensional noise, the sampled offset value will change over time. This helps break up the uniformity and predictability of the previous solution.

Unfortunately, we have lost one important property of the previous solution: The fact that the maximum offset was directly proportional to the distance from the HMD. We could try to reintroduce proportionality naively by multiplying the sample by the distance  $r$ :

$$s' := r \cdot s \begin{pmatrix} f_s x \\ f_s y \\ f_s z \\ f_t t \end{pmatrix} \quad (1.3)$$

By this modification, we have effectively changed the amplitude of the noise, yet the frequency remains the same – and uniform. If we were to use this sample  $s'$  as the distance offset, we would cause distant geometry to self-intersect. Therefore, a different solution is needed.

For this task, we may use fractional Brownian motion (**fBm**). Before we go into how **fBm** can help resolve this issue, let's briefly describe how it is used in the synthesis of self-similar noise. **fBm** is a technique of combining layers of noise,

while varying their amplitudes and frequencies.

$$s' := \frac{1}{k} \sum_{i=0}^{k-1} g^i \cdot s \left( l^i \begin{bmatrix} f_s x \\ f_s y \\ f_s z \\ f_t t \end{bmatrix} + i \vec{o} \right) \quad (1.4)$$

In equation 1.4, we combine  $k \in \mathbb{N}$  layers of simplex noise. The parameter  $g \in \mathbb{R}$  (gain) changes the amplitude of each layer, and the parameter  $l \in \mathbb{R}$  (lacunarity) changes the frequency of each layer. Typically,  $l = \frac{1}{g}$ ; in that case, we are generating so-called “pink noise”. The parameter  $\vec{o} \in \mathbb{R}^n$  is a coordinate offset applied to each layer, to break up symmetry (a different seed for each layer could also be used).

Now, back to our original problem of keeping the amplitude proportional to the distance from the HMD. Instead of using  $k$  layers of noise with indices  $i = 0, 1, \dots, k - 1$ , we can offset the indices by an integer value depending on the distance from the HMD. If we do so carefully, we will recover the direct proportionality. We define a real-valued offset  $m: \mathbb{R} \rightarrow \mathbb{R}$ :

$$m(r) = \log_a r \quad (1.5)$$

Where  $a \in \mathbb{R}$  is a parameter; more on this later. Then, we can define the rounded-down integer part  $j: \mathbb{R} \rightarrow \mathbb{Z}$  to offset the layer indices with:

$$j(r) = \lfloor m(r) \rfloor \quad (1.6)$$

$$s' := \frac{1}{k} \sum_{i=0}^{k-1} g^{i+j(r)} \cdot s \left( l^{i+j(r)} \begin{bmatrix} f_s x \\ f_s y \\ f_s z \\ f_t t \end{bmatrix} + (i + j(r)) \vec{o} \right) \quad (1.7)$$

Equation 1.7 differs from equation 1.4 in that we have added an index offset  $j(r)$ , which is computed from the distance to the HMD  $r$ . Now we are able to offset the indices. However, this will result in noticeable discontinuities of the noise at the discontinuities of  $j(r)$ .

In order to remove these discontinuities, we shall introduce blending. Let us refer to the layers at indices  $j(r), j(r) + 1, \dots, j(r) + k - 1$  as “active layers”, the layer at index  $j(r)$  as “the first active layer” and the layer at index  $j(r) + k - 1$  as “the last active layer”.

Let us define a weight function  $w: \mathbb{Z} \times \mathbb{R} \rightarrow [0; 1]$ , which will attenuate the first

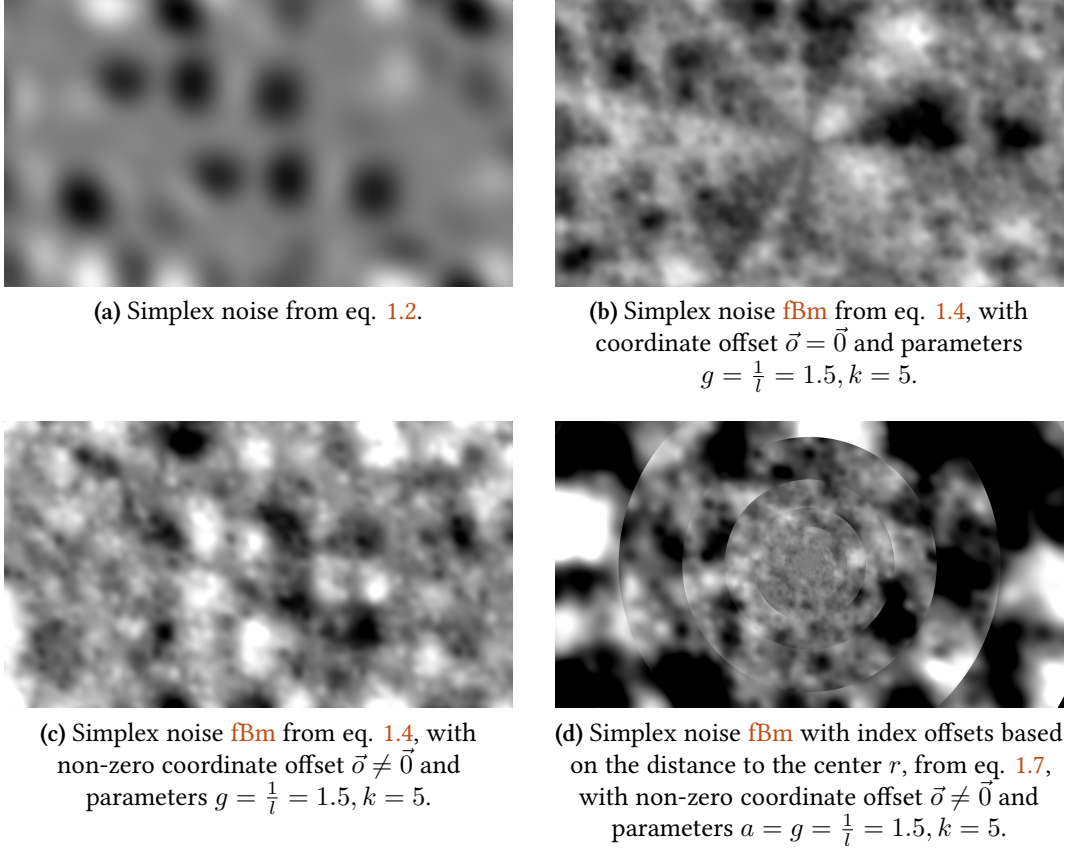


**Figure 1.4:** Intermediate steps in the construction of the blended fBm noise. Amplitude adjusted for visualization.

and last active layer, while leaving other layers unaffected.

$$w(i, r) = \begin{cases} m(r) - j(r) = \{m(r)\} & \text{if } i = 0 \\ 1 - (m(r) - j(r)) = 1 - \{m(r)\} & \text{if } i = k \\ 1 & \text{otherwise} \end{cases} \quad (1.8)$$

Where  $\{x\} = x - \lfloor x \rfloor$  is the upper fractional part of  $x$ .

$$s' := \frac{1}{k} \sum_{i=0}^k w(i, r) \cdot g^{i+j(r)} \cdot s \left( l^{i+j(r)} \begin{bmatrix} f_s x \\ f_s y \\ f_s z \\ f_t t \end{bmatrix} + (i + j(r)) \vec{o} \right) \quad (1.9)$$

Besides multiplying each layer by the weight  $w(i, r)$ , we have also changed the upper index of the sum from  $k - 1$  to  $k$ , to account for the attenuation.

We have arrived at the derived general equation for blended fBm noise based on distance  $r$  with parameters  $a, g, l \in \mathbb{R}; \vec{o} \in \mathbb{R}^n; k \in \mathbb{N}$ . However, in general, this

form does not satisfy our requirement of the amplitude being proportional to the distance  $r$ . In order for that to be true, we must set  $a = g = \frac{1}{l}$ .

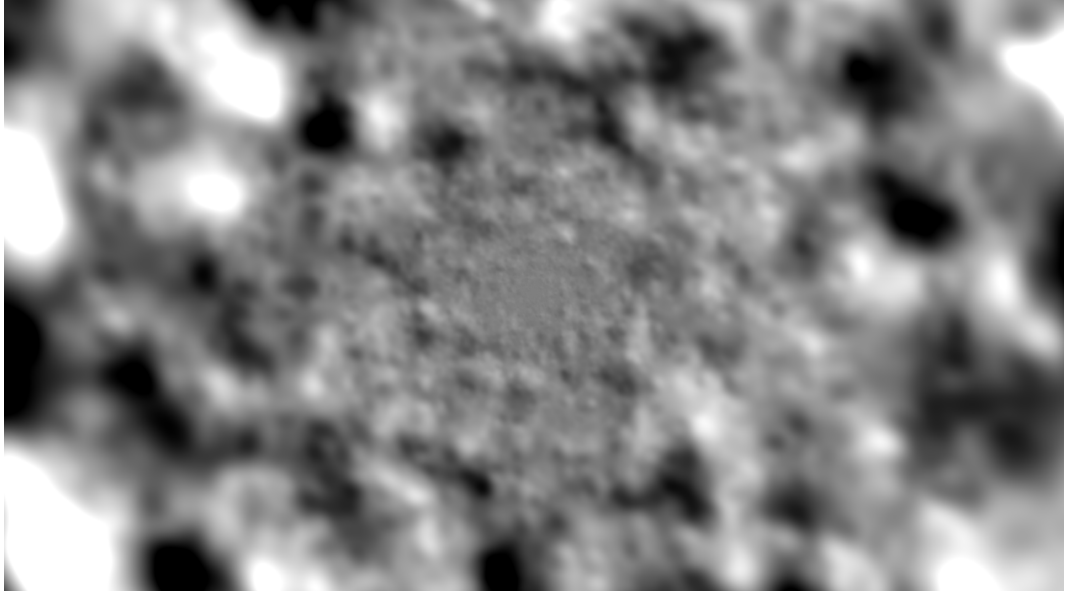


**Figure 1.5:** The final implementation of the blended fBm Simplex noise based on the distance to the center  $r$ , from eq. 1.12, with non-zero coordinate offset  $\vec{o} \neq \vec{0}$  and parameters  $a = g = \frac{1}{l} = 1.5$ ,  $k = 5$ . Amplitude adjusted for visualization.

The equation then expands to:

$$s' := \frac{1}{k} \sum_{i=0}^k w(i, r) \cdot a^{i+\lfloor \log_a r \rfloor} \cdot s \left( a^{-(i+\lfloor \log_a r \rfloor)} \begin{bmatrix} f_s x \\ f_s y \\ f_s z \\ f_t t \end{bmatrix} + (i + j(r)) \vec{o} \right) \quad (1.10)$$

$$w(i, r) = \begin{cases} \{\log_a r\} & \text{if } i = 0 \\ 1 - \{\log_a r\} & \text{if } i = k \\ 1 & \text{otherwise} \end{cases} \quad (1.11)$$

Finally, we may or may not want the frequency of the fourth coordinate to be influenced by lacunarity. We reached better results when lacunarity did not affect the time coordinate.

$$s' := \frac{1}{k} \sum_{i=0}^k w(i, r) \cdot a^{i+\lfloor \log_a r \rfloor} \cdot s \left( \begin{bmatrix} a^{-(i+\lfloor \log_a r \rfloor)} f_s x \\ a^{-(i+\lfloor \log_a r \rfloor)} f_s y \\ a^{-(i+\lfloor \log_a r \rfloor)} f_s z \\ f_t t \end{bmatrix} + (i + j(r)) \vec{o} \right) \quad (1.12)$$

This is the final equation used to sample blended fBm noise based on the distance  $r$  with parameters  $a \in \mathbb{R}$ ,  $\vec{o} \in \mathbb{R}^n$ ,  $k \in \mathbb{N}$ . This equation is used in the application

to displace vertices of scene geometry. The result is scaled to ensure that no self-intersections of scene geometry occur.

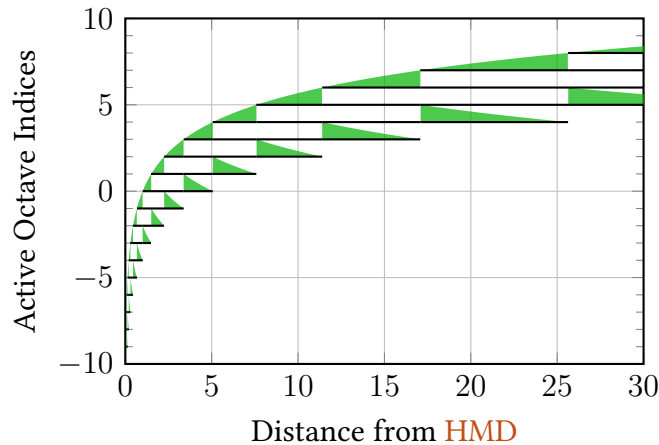


**Figure 1.6:** Computation of active octaves based on the distance from the **HMD**. Active octaves as solid black lines. Green areas correspond to the weight of the first and last currently active octave.

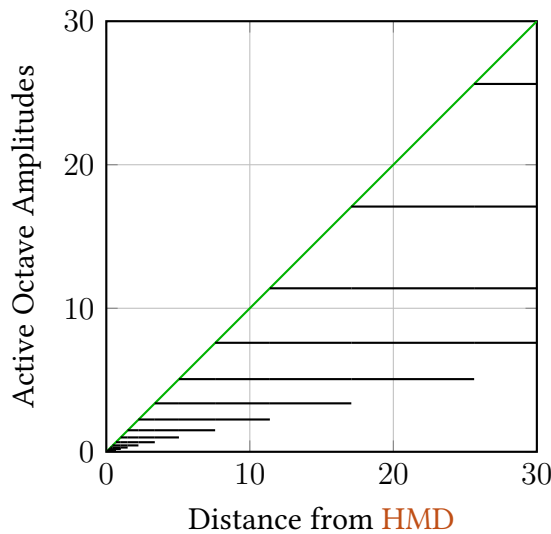


**Figure 1.7:** Amplitudes of active octaves based on the distance from the **HMD**, for the case where  $a = g = 1.5$ . Active octaves as solid black lines. The green line shows the direct proportionality of the maximum active octave amplitude and the distance from the **HMD**.

### 1.2.1.2 Visual Drifting

(Díaz 2010; Kleinman, Gillin, and Wyatt 1977)

### 1.2.2 Non-Spatial Effects

#### 1.2.2.1 Visual Acuity Enhancement

(Heinrich Klüver 1942; Klüver 1966; Dittrich 1998; Díaz 2010; Siegel and Jarvik 1975; Fischer, Hill, and Warshay 1969)

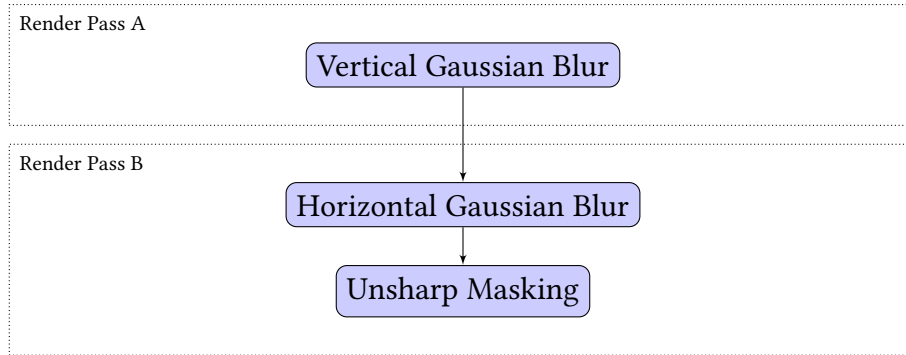


Figure 1.8: Execution order of distinct components of the sharpening effect.

#### 1.2.2.2 Tracers

(Hartman and Hollister 1963; Díaz 2010; Anderson and O’Malley 1972; Kleinman, Gillin, and Wyatt 1977)

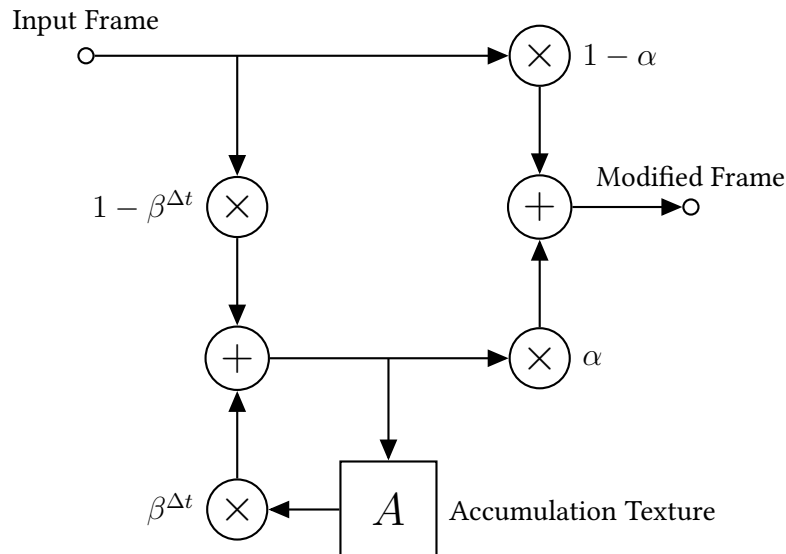
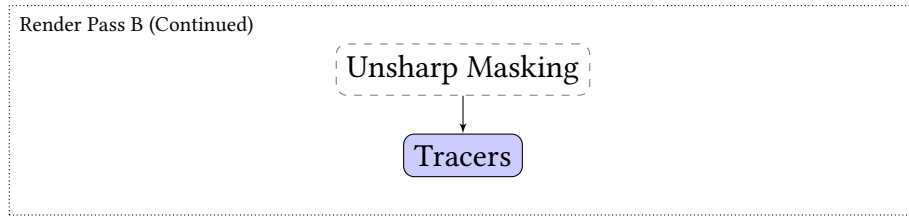


Figure 1.9: Execution graph of the tracer effect. The parameter  $\alpha \in [0; 1]$  is the total opacity of the effect. The parameter  $\beta \in [0; 1]$  is the feedback modifier corresponding to the “duration” of the resulting blur. Finally,  $\Delta t$  is the time since the previous frame, making the effect less influenced by framerate fluctuations.



**Figure 1.10:** The tracer effect is applied in the second render pass of the sharpening effect.

## 1.3 Complex Replication

### 1.3.1 Execution Order

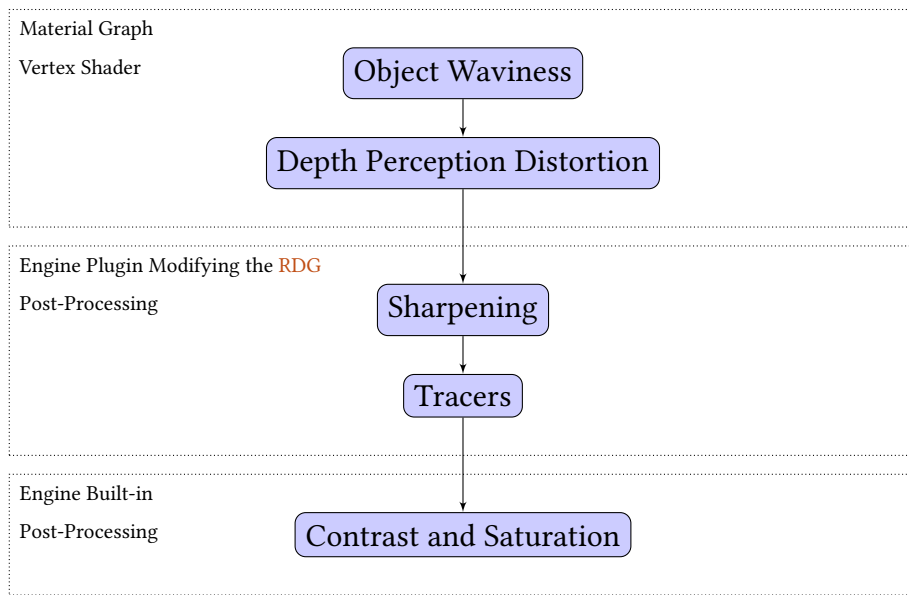


**Figure 1.11:** The execution order of partial replications, making up the complex replication.

### 1.3.2 Experiment Automation

## List of Acronyms

**11-ASC** 11-Factor Altered States of Consciousness Questionnaire: A version of the *Altered States of Consciousness Rating Scale* psychometric questionnaire, which is based on the hypothesis that ASCs have a common core independent of the induction method which distinguishes them from the waking conscious state (Figueiredo et al. 2016; Studerus, Gamma, and Vollenweider 2010).

**5-HT** 5-hydroxytryptamine, also known as serotonin

**5D-ASC** 5-Dimensional Altered States of Consciousness Questionnaire: Like the 11-Factor Altered States of Consciousness Questionnaire (**11-ASC**), but with different scoring and categories (Dittrich, Lamparter, and Maurer 2010).

**AI** artificial intelligence

**ASC** altered state of consciousness: See section ?? for a complete definition and related terms.

**CPU** central processing unit

**DCNN** deep convolutional neural networks

**DMT** *N,N*-dimethyltryptamine: A classical hallucinogenic drug first synthesized in 1931 (Manske 1931), a psychoactive compound of Ayahuasca, the ceremonial spiritual medicine used by Amazonian natives for shamanic purposes and to bond socially in a casual setting (Mark Hay 2020).

**DSP** digital signal processing

**EEG** electroencephalograph

**FOV** field of view

**FPS** frames per second: A unit of monitor refresh rate, equivalent to hertz (Hz).

**GLSL** OpenGL Shading Language: A shading language used by the OpenGL graphics API.

**GPU** graphics processing unit: A specialized extension module providing acceleration for computer graphics computations and other parallelizable tasks.

**HDRI** high dynamic range imaging

**HLSL** High Level Shading Language: A shading language used by the DirectX graphics API.

**HMD** head-mounted display

**LSD** lysergic acid diethylamide: A classical hallucinogenic drug first synthesized in 1938 from ergotamine, an alkaloid of the ergot rye fungus (Albert Hofmann 1969).

**MEQ30** 30-item revised mystical experience questionnaire

**MTE** ‘mystical-type’ experience: Subjective experiences whose characteristics include a sense of connectedness, transcendence, and ineffability.

**PCI** Phenomenology of Consciousness Inventory: A psychometric questionnaire based on the hypothesis that different states of consciousness can be characterized in terms of phenomenological dimensions which can be quantified in terms of their intensity. The resulting pattern is assumed to be typical of a particular induction method and can be observed consistently (Figueiredo et al. 2016).

**RAM** random-access memory

**RDG** Rendering Dependency Graph: A graphics rendering execution graph of UE4.

**THC** tetrahydrocannabinol: One of the psychoactive compounds in cannabis.

**UE4** Unreal Engine 4: A game development engine.

**VAS** visual analog scale

**VR** virtual reality

**fBm** fractional Brownian motion

# Bibliography

- Albert Hofmann. 1969. "LSD: Completely Personal." Accessed December 6, 2013. <https://web.archive.org/web/20131206032629/http://www.maps.org/newsletters/v06n3/06346hof.html>.
- Alessa Baker. 2021. "CustomShaderDirectoryExample: An example project for a tutorial on adding a custom shader directory." Accessed May 18, 2022. <https://github.com/Sythenz/CustomShaderDirectoryExample>.
- Anderson, WH, and John E O'Malley. 1972. "Trifluoperazine for the trailing phenomenon." *JAMA* 220 (9): 1244–1245.
- Dittrich, Adolf. 1998. "The standardized psychometric assessment of altered states of consciousness (ASCs) in humans." *Pharmacopsychiatry* 31 (S 2): 80–84.
- Dittrich, Adolf, Daniel Lamparter, and Maja Maurer. 2010. "5D-ASC: Questionnaire for the assessment of altered states of consciousness." *A short introduction. Zurich, Switzerland: PSIN PLUS*.
- Díaz, José Luis. 2010. "Sacred plants and visionary consciousness." *Phenomenology and the Cognitive Sciences* 9 (2): 159–170.
- Figueiredo, Renato Garita, Hendrik Berkemeyer, Katharina Dworatzky, and Timo T Schmidt. 2016. "Building a unifying database to enable flexible meta-analyses of data on altered states of consciousness."
- Fischer, Rico, RM Hill, and Diana Warshay. 1969. "Effects of the psychodysleptic drug psilocybin on visual perception. Changes in brightness preference." *Experientia* 25 (2): 166–169.
- Fischer, Roland, Richard Hill, Karen Thatcher, and James Scheib. 1970. "Psilocybin-induced contraction of nearby visual space." *Agents and actions* 1 (4): 190–197.
- Hartman, Alan M, and Leo E Hollister. 1963. "Effect of mescaline, lysergic acid diethylamide and psilocybin on color perception." *Psychopharmacologia* 4 (6): 441–451.
- Hill, Richard M, and Roland Fischer. 1973. "Induction and extinction of psilocybin induced transformations of visual space." *Pharmacopsychiatry* 6 (04): 258–263.

- Hill, RM, Roland Fischer, and Diana Warshay. 1969. "Effects of excitatory and tranquilizing drugs on visual perception. Spatial distortion thresholds." *Experientia* 25 (2): 171–172.
- Kleinman, Joel Edward, John Christian Gillin, and Richard Jed Wyatt. 1977. "A comparison of the phenomenology of hallucinogens and schizophrenia from some autobiographical accounts." *Schizophrenia Bulletin* 3 (4): 560.
- Klüver, H. 1966. *Mescal and mechanisms of hallucinations Chicago*.
- Klüver, Heinrich. 1942. "Mechanisms of hallucinations."
- Kometer, Michael, and Franz X Vollenweider. 2016. "Serotonergic hallucinogen-induced visual perceptual alterations." *Behavioral neurobiology of psychedelic drugs*: 257–282.
- Madary, Michael, and Thomas K Metzinger. 2016. "Real virtuality: a code of ethical conduct. Recommendations for good scientific practice and the consumers of VR-technology." *Frontiers in Robotics and AI* 3:3.
- Manske, Richard HF. 1931. "A synthesis of the methyltryptamines and some derivatives." *Canadian Journal of Research* 5 (5): 592–600.
- Mark Hay. 2020. "The Colonization of the Ayahuasca Experience." Accessed February 7, 2022. <https://web.archive.org/web/20220207102112/https://daily.jstor.org/the-colonization-of-the-ayahuasca-experience/>.
- Olano, Mark, John C Hart, Wolfgang Heidrich, Bill Mark, and Ken Perlin. 2002. "Real-time shading languages." SIGGRAPH.
- Perlin, Ken. 1985. "An image synthesizer." *ACM Siggraph Computer Graphics* 19 (3): 287–296.
- Preller, Katrin H, and Franz X Vollenweider. 2016. "Phenomenology, structure, and dynamic of psychedelic states." *Behavioral neurobiology of psychedelic drugs*: 221–256.
- Siegel, Ronald K, and Murray E Jarvik. 1975. "Drug-induced hallucinations in animals and man." *Hallucinations: Behavior, experience and theory* 81:161.
- Studerus, Erich, Alex Gamma, and Franz X Vollenweider. 2010. "Psychometric evaluation of the altered states of consciousness rating scale (OAV)." *PloS one* 5 (8): e12412.